

## Core Spectra of Metals

Coenraad A. Swarts,<sup>(a)</sup> John D. Dow, and C. P. Flynn*Department of Physics and Materials Research Laboratory, University of Illinois at Urbana-Champaign, Urbana, Illinois 61801*

(Received 2 April 1979)

By means of model calculations for an independent-electron metal, we calculate the photon absorption and emission spectra of core states, including conduction-electron relaxation. We find an x-ray edge anomaly merging into a spectrum resembling that of screened-exciton theory. Neither of these theoretical limits adequately represents the detailed structure of the exact results.

This Letter reports exact solutions of a model for x-ray absorption and emission in metals. Recent attention to core spectra of metals has focused on the threshold anomaly caused by the conduction-electron response to the suddenly changed core field. This anomaly has been discussed by Nozières and de Dominicis (ND)<sup>1</sup> and other workers,<sup>2</sup> using many-body methods for very large numbers of conduction electrons. Our approach is to solve the same model exactly for small numbers of conduction electrons ( $\lesssim 10^6$ ) using Slater determinants.<sup>3</sup> As in recent investigations of x-ray photoelectron spectra (XPS) by similar methods,<sup>3</sup> the absorption and emission profiles are insensitive to the size of the metal. The present results show departures from the ND asymptotic result for the threshold anomaly within  $\lesssim 0.03E_F$  of the threshold itself ( $E_F$  is the Fermi energy). The main features of the spectra arise from the perturbed density of one-electron states in the central cell, and can be represented with fair accuracy for weak final-state interactions by an analog of Elliott exciton theory.<sup>4,5</sup>

We start with the ND initial-state Hamiltonian

$$H_i = \sum_{j=1}^N \frac{p_j^2}{2m} + U(r_j) \quad (1)$$

and the final-state Hamiltonian

$$H_f = \sum_{j=1}^{N+1} \frac{p_j^2}{2m} + U(r_j) + V(r_j) \quad (2)$$

for the conduction electrons.  $U$  is the one-body potential near the central cell in the ground state and  $U+V$  the potential in the final state. The absorption process injects a core electron into the conduction band; the summations over momenta,  $p_j$ , and one-body potentials therefore run over  $N$  electrons in the ground state and  $N+1$  electrons in the excited state.  $V(r_j)$  is the one-body final-state interaction introduced by the core hole. For emission,  $H_i$  and  $H_f$  are reversed. We follow ND further in neglecting exchange between the core hole and the conduction band; the ground- and ex-

cited-state wave functions are then  $\varphi_c \Phi$  and  $\Psi$ ;  $\varphi_c$  is the core orbital;  $\Phi$  is the Slater determinant of the  $N$ -band one-electron eigenfunctions  $\varphi_j$  of  $H_i$ ; and  $\Psi$  is the determinant of the  $N+1$  eigenfunctions  $\psi_i$  of  $H_f$ .

It will suffice to investigate a core  $p$  level of very small radius  $a_c$ .<sup>6</sup> The optical matrix element  $\langle i|M|fn\rangle$  connecting the initial Slater determinant  $|i\rangle$  to a particular final configuration  $|fn\rangle$  is then

$$\langle i|M|fn\rangle = \mathfrak{M} \begin{vmatrix} \psi_1(0) & \psi_2(0) & \cdots & \psi_{N+1}(0) \\ (\varphi_1, \psi_1) & (\varphi_1, \psi_2) & \cdots & (\varphi_1, \psi_{N+1}) \\ \vdots & \vdots & & \vdots \\ (\varphi_N, \psi_1) & (\varphi_N, \psi_2) & \cdots & (\varphi_N, \psi_{N+1}) \end{vmatrix}, \quad (3)$$

with  $\mathfrak{M} = (\varphi_c | \vec{r} | \psi_k) / \psi_k(0)$ .<sup>6</sup> The absorption profile is

$$K(E) = |\mathfrak{M}|^2 K(E) = \sum_n |\langle i|M|fn\rangle|^2 \delta(E - E_{fn} + E_i + E_0). \quad (4)$$

Here  $E_0$  is the excitation threshold energy;  $E_{fn}$  and  $E_i$  are the total energies of the final and initial  $(N+1)$ -particle states. In a spherically symmetrical system the one-particle overlap matrix elements  $(\psi, \varphi)$  are zero for unlike angular momenta, and the profile (4) is therefore a convolution of independent contributions from different angular momenta. Here we confine attention to the physically interesting optical channel and consider only  $s$ -wave band states in a single spin channel.

The spectra are computed as follows: The Fermi wave vector (and hence the electron density) is chosen, the gas is enclosed in a box of radius  $R = N\pi/k_F$ , the orbitals  $\varphi_j$  and  $\varphi_k$  are determined for the chosen  $U$  and  $V$ , the determinants  $\langle i|M|fn\rangle$  are computed for various final states  $|fn\rangle$ , and the spectra are evaluated for  $N = 5, 10, 20, 40$ ,

and 80 s waves.<sup>3</sup> For  $N=80$  the spectra become sensibly independent of  $N$ , other than for the energy resolution  $\delta E \sim 2E_F/N$ . This may be removed by a Gaussian convolution of width comparable with the level spacing  $\delta E$ , or by fitting the integrated profile and differentiating the fit.

A square-well "electron-hole interaction"  $V(r)$  provides a reasonable compromise between simplicity and realism. The results shown in Fig. 1 for various strengths of  $V$  arbitrarily employ a radius  $a$  with  $k_F a = 0.73$  (i.e.,  $a/r_s \approx 0.38$  for Na) and  $U=0$  to simulate absorption in the perfect free-electron metal. The calculated absorption is indicated by a solid line at  $E > 0$ , and the corresponding emission at  $E < 0$ , the zero of energy being at the common threshold. To indicate the magnitude of  $V$  we label the results by  $\delta_0$ , the change of s-wave phase shift caused by  $V$  at the Fermi energy  $E_F$ . Some observed spectra resemble Figs. 1(a) and 1(b).

The most striking result of the calculations is that for both absorption and emission with  $\delta_0 < 0.25\pi$  in the broad trend of the results is well represented by the simple screened-exciton approximation<sup>5</sup> indicated by the broken line in Fig. 1. This approximation replaces all effects of the additional excited-state potential by a multiplicative enhancement factor  $|\psi(0)/\varphi(0)|^2$  for states of the relevant energy. Deviations from the screened-exciton prescription are most pronounced near threshold where the x-ray anomaly is clearly evident, and, in emission, above the band bottom where the sum rule on oscillator strength (see below) causes a depletion of emission that compensates the enhancement by the emission edge anomaly. For  $\delta_0 \gtrsim 0.25\pi$  the screened-exciton model differs markedly from the exact emission results.

Clearly apparent in Fig. 1 is the x-ray threshold anomaly discussed by Nozières and de Dominicis. This arises from interferences inherent in the determinantal wave functions, as demonstrated by Friedel.<sup>7</sup> The chain lines in the figures show the asymptotic threshold profiles predicted by the ND one-channel result:  $|E|^{-\alpha_0}$ , with  $\alpha_0 = 2\delta_0/\pi - (\delta_0/\pi)^2$ . These results are correctly normalized by procedures given elsewhere.<sup>3, 8</sup> The ND profile has been widely used in analyses of experimental data, but has never been previously subjected to quantitative theoretical evaluation. The present calculations show that the range throughout which this approximation remains quantitatively accurate is limited to energies within  $\lesssim 0.03E_F$  of threshold; for typical metals with

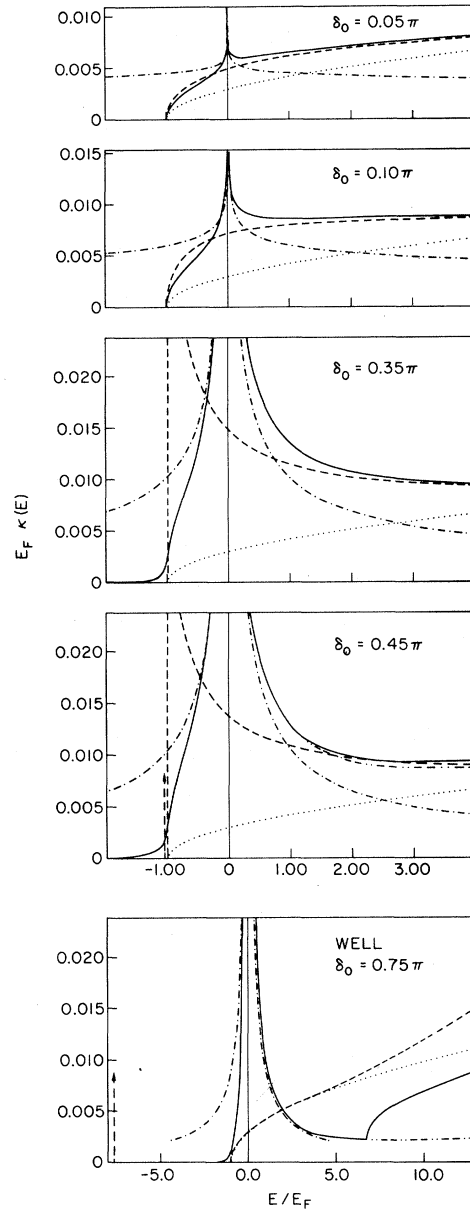


FIG. 1. Core spectra for a square-well final-state interaction  $V$  of increasing strength (or specified by  $\delta_0/\pi$ ). The units of energy and length are the Rydberg and Bohr radius. Absorption (emission) is given for  $E > 0$  ( $E < 0$ ). Solid lines: present work; broken lines: screened exciton approximation; bound excitons are indicated by arrows; dotted lines: free electron approximation; dash-dot lines: asymptotic ND theory; double dash, double dot: contribution of first threshold to line shape to beyond the second threshold.

$E_F \sim 5$  eV this range of validity is considerably less than the experimental energy range ( $\sim 1$  eV) over which typical attempts to fit data have been employed. A similar limitation holds for XPS

spectra.<sup>3</sup> The present exact results show that threshold exponents extracted using such fitting procedures can have, at best, a semiquantitative significance.

The conclusions stated above do not appear to depend on details of the "core potential." Differing potentials that give the same value of  $\delta_0$  produces widely different spectra. Figure 2 shows as solid lines the spectra calculated for  $\delta$ -shell, barrier, and square-well potentials, with  $U$  repulsive or  $V$  attractive, but each corresponding to  $\delta_0 = 0.25\pi$ , with  $\delta_0$  a positive phase-shift change accompanying absorption. In all cases the screened-exciton approximation to the oscillator strength in absorption well above threshold serves quite adequately (broken lines). The edge anomaly does appear in all the spectra, but with widely differing strengths and in no case conforming adequately to the asymptotic ND form (chain lines) beyond  $\sim 0.03E_F$ . These are the first results that show the full diversity of the core excitation process in metals. It is apparent that even within the independent-particle model there exists a complex blending of one-electron and x-

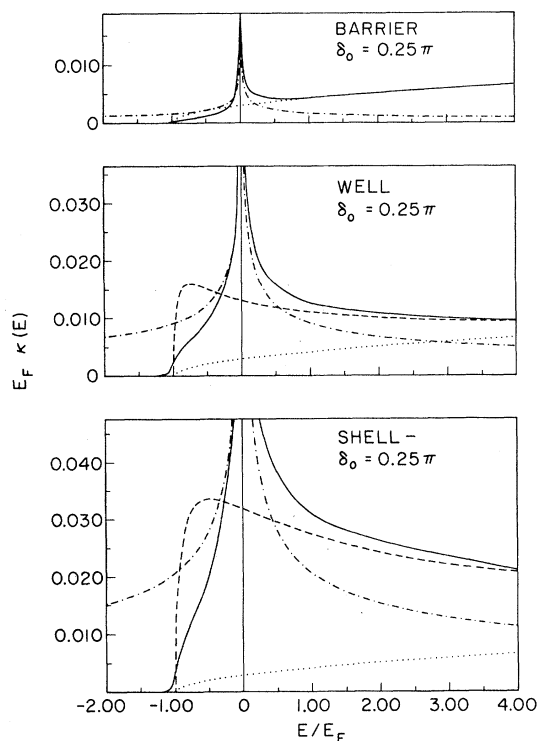


FIG. 2. Comparison of core spectra for different final-state interactions: (a)  $U = \infty$  for  $r < a$ ,  $U = 0$  for  $r > a$ , and  $U + V = 0$ . Lines as in Fig. 1. (b)  $V = -V_0$  for  $r > a$ , and  $U = 0$ . (c)  $V = -V_0 \delta(r - a)$  and  $U = 0$ .

ray edge phenomena that neither of these limiting theories reproduces in a realistic way.

The exact absorption and emission profiles are not mirror images. Similar mirror asymmetries have been reported for Li,<sup>9</sup> Na,<sup>10</sup> and K.<sup>11</sup> In fact, the emission strength decays rapidly near  $E_F$  in order to compensate the enhancement at the edge itself.

Note also that the evolution of a bound state, and the formation of a second absorption threshold associated with the empty bound state in the excited configuration, may be traced in Fig. 1 as  $\delta_0/\pi$  passes from 0.25 through 0.45 to 0.75. The asymptotic power-law behavior predicted by Combescot and Nozières for this second threshold<sup>12</sup> has a similar range of validity to that at the primary threshold.

Certain independent checks have verified the results of these calculations. The emission sum rule<sup>13</sup>

$$\int_{-\infty}^0 K(E) dE = \sum_{i=1}^N |\psi_i(0)|^2 \quad (5)$$

agrees accurately with the calculated results. No such sum rule constrains absorption because the core radius is presumed in Eq. (2) to be arbitrarily small. In practice,  $K(E)$  for finite core radii decays below its zero-core-radius value at high energies.<sup>6</sup>

In summary, the exactly calculated model excitation profiles depend significantly on the core-hole potential. They exhibit gross features of both screened-exciton theory and the ND edge structure. Neither theory alone represents the exact profiles well for realistic electron-hole interaction strengths.

It is possible that by appropriate modeling of one-particle potentials, the present methods could be used to predict accurate x-ray spectra for real metals. However, the ND model used here applies only to independent particles suddenly perturbed by a one-body potential. The inclusion of electron-electron interactions within this framework has been widely discussed,<sup>14</sup> but these complexities have not yet been incorporated into comprehensive calculations of core line shapes for metals.

We gratefully acknowledge the support of the University of Illinois Materials Research Laboratory and the U. S. Department of Energy, under Contract No. DOE EY-76-C-02-1198.

(a) Present address: Department of Applied Physics, California Institute of Technology, Pasadena, Calif.

91103.

<sup>1</sup>P. Nozières and C. T. de Dominicis, *Phys. Rev.* **173**, 1097 (1969).

<sup>2</sup>For reviews of the theory, see J. J. Hopfield, *Comments Solid State Phys.* **2**, 40 (1969); G. D. Mahan, *Solid State Phys.* **29**, 75 (1974); J. D. Dow, *Comments Solid State Phys.* **6**, 71 (1975). For a finite-band model see V. I. Grebennikov, Yu. A. Babanov, and O. B. Sokolov, *Phys. Status Solidi (b)* **79**, 423 (1977), and **80**, 73 (1977).

<sup>3</sup>J. D. Dow and C. P. Flynn, to be published; note that  $N=80$   $s$  waves corresponds to  $N > 10^6$  electrons.

<sup>4</sup>R. J. Elliott, *Phys. Rev.* **108**, 1384 (1957).

<sup>5</sup>J. D. Dow, *J. Phys. F* **5**, 1113 (1975).

<sup>6</sup>As in exciton theory, the matrix element  $\mathfrak{M}$  depends on the core-hole radius  $a_c = a_{\text{Bohr}}/Z_{\text{eff}}$  for a hydrogenic  $2p$  core, we have  $\mathfrak{M} \propto a_c^5$ . The small-core approximation to the shape of the line is valid for all energies such that  $ka_c \ll 1$ , where  $\hbar^2 k^2/2m$  is the kinetic energy of the optical electron. The falloff occurs at an electron energy  $\sim Z_{\text{eff}}^2$  Rydbergs.

<sup>7</sup>J. Friedel, *Philos. Mag.* **43**, 153, 1115 (1952); *Com-*

*ments Solid State Phys.* **2**, 21 (1969).

<sup>8</sup>C. A. Swarts, Ph.D. thesis, University of Illinois, 1979 (unpublished), Chap. 3.

<sup>9</sup>T. A. Callcott, E. T. Arakawa, and D. L. Ederer, *Phys. Rev. B* **16**, 5185 (1977); T. A. Callcott and E. T. Arakawa, *Phys. Rev. Lett.* **38**, 442 (1977).

<sup>10</sup>T. A. Callcott, E. T. Arakawa, and D. L. Ederer, *Phys. Rev. B* **18**, 6622 (1978).

<sup>11</sup>T. Ichii, Y. Sakisaka, S. Yamaguchi, T. Hanyu, and H. Ishii, *J. Phys. Soc. Jpn.* **42**, 876 (1977); P. R. Norris, *Phys. Lett.* **45A**, 387 (1973).

<sup>12</sup>M. Combescot and P. Nozières, *J. Phys. (Paris)* **32**, 913 (1971).

<sup>13</sup>This is easily derived by expanding the determinant of Eq. (3) with respect to the first row and summing all possible final states; Eq. (5) then follows immediately from the completeness of the final states.

<sup>14</sup>P. Longe, *Phys. Rev. B* **8**, 2572 (1973); C. P. Flynn, *Phys. Rev. B* **14**, 5254 (1976); P. Minnhagen, *Phys. Lett.* **56A**, 327 (1976); E. A. Stern, S. M. Heald, and B. Bunker, to be published; T. A. Carlson and M. V. Krause, *Phys. Rev.* **140**, A1057 (1965).

## Time-Resolved Optical Absorption and Mobility of Localized Charge Carriers in $\alpha$ -As<sub>2</sub>Se<sub>3</sub>

Joseph Orenstein and Marc Kastner

*Department of Physics and Center for Materials Science and Engineering,  
Massachusetts Institute of Technology, Cambridge, Massachusetts 02139*

(Received 16 February 1979)

The first measurements are reported of simultaneous, transient, photoinduced optical absorption (PA) and photoconductivity (PC) in an amorphous semiconductor ( $\alpha$ -As<sub>2</sub>Se<sub>3</sub>). Measurements in the time range 100 ns to 1 ms show that the same density of excited carriers gives rise to both effects. PA is observed only when carriers are in localized states, whereas PC is observed for both hot carriers ( $\mu\tau \approx 7 \times 10^{-12}$  cm<sup>2</sup> V<sup>-1</sup>) and localized carriers.

The concept of localized states with an effective negative correlation energy<sup>1</sup> has explained a long-standing puzzle in the study of chalcogenide glasses, namely the pinning of the Fermi level in the absence of electron spin paramagnetism. Recent models<sup>2,3</sup> have applied this concept to specific bond-coordination defects in the glass structure in order to explain not only the diamagnetic ground state but a wide variety of excited-state phenomena as well. Of these phenomena, carrier transport and photoinduced ESR and optical absorption are thought to be direct probes of the density, structure, and charge of these defects.

In  $\alpha$ -As<sub>2</sub>Se<sub>3</sub>, the best characterized of the compound chalcogenide glasses, a trap-limited carrier transport mechanism has been proposed<sup>4,5</sup> to account for the large,  $\sim 0.6$  eV, activation en-

ergy of the hole drift mobility. The defect models identify this hole trap with the singly coordinated defect which is negatively charged in its ground state. The ESR signal and optical absorption band which appear together during illumination at low temperatures<sup>6</sup> are thought to result from photoionization of the bound electron pair at this same localized state. In recently reported experiments,<sup>7</sup> however, measurements of carrier transport and photoinduced ESR and absorption failed to show the expected correlation.

The drift mobility and photoinduced spin density were measured in samples of  $\alpha$ -As<sub>2</sub>Se<sub>3</sub> which were doped with a variety of impurities. Several elements (e.g., Tl, I) changed the hole mobility while leaving its activation energy the same as that in the undoped material, strongly suggesting